

# Acute Synthesis of CPEB Is Required for Plasticity of Visual Avoidance Behavior in *Xenopus*

Wanhua Shen,<sup>1,2</sup> Han-Hsuan Liu,<sup>2,4</sup> Lucio Schiapparelli,<sup>2</sup> Daniel McClatchy,<sup>3</sup> Hai-yan He,<sup>2</sup> John R. Yates III,<sup>3</sup> and Hollis T. Cline<sup>2,3,4,\*</sup>

<sup>1</sup>Key Lab of Organ Development and Regeneration of Zhejiang Province, College of Life and Environmental Sciences, Hangzhou Normal University, Hangzhou, Zhejiang 310036, China

<sup>2</sup>The Dorris Neuroscience Center, Department of Molecular and Cellular Neuroscience, The Scripps Research Institute, 10550 North Torrey Pines Road, La Jolla, CA 92037, USA

<sup>3</sup>Department of Chemical Physiology, The Scripps Research Institute, 10550 North Torrey Pines Road, La Jolla, CA 92037, USA

<sup>4</sup>Kellogg School of Science and Technology, The Scripps Research Institute, 10550 North Torrey Pines Road, La Jolla, CA 92037, USA

\*Correspondence: [cline@scripps.edu](mailto:cline@scripps.edu)

<http://dx.doi.org/10.1016/j.celrep.2014.01.024>

This is an open-access article distributed under the terms of the Creative Commons Attribution-NonCommercial-No Derivative Works License, which permits non-commercial use, distribution, and reproduction in any medium, provided the original author and source are credited.

## SUMMARY

Neural plasticity requires protein synthesis, but the identity of newly synthesized proteins generated in response to plasticity-inducing stimuli remains unclear. We used in vivo bio-orthogonal noncanonical amino acid tagging (BONCAT) with the methionine analog azidohomoalanine (AHA) combined with the multidimensional protein identification technique (MudPIT) to identify proteins that are synthesized in the tadpole brain over 24 hr. We induced conditioning-dependent plasticity of visual avoidance behavior, which required N-methyl-D-aspartate (NMDA) and Ca<sup>2+</sup>-permeable  $\alpha$ -Amino-3-hydroxy-5-methyl-4-isoxazolepropionic acid (AMPA) receptors,  $\alpha$ CaMKII, and rapid protein synthesis. Combining BONCAT with western blots revealed that proteins including  $\alpha$ CaMKII, MEK1, CPEB, and GAD65 are synthesized during conditioning. Acute synthesis of CPEB during conditioning is required for behavioral plasticity as well as conditioning-induced synaptic and structural plasticity in the tectal circuit. We outline a signaling pathway that regulates protein-synthesis-dependent behavioral plasticity in intact animals, identify newly synthesized proteins induced by visual experience, and demonstrate a requirement for acute synthesis of CPEB in plasticity.

## INTRODUCTION

Synaptic plasticity is thought to be a cellular substrate for experience-dependent behavioral plasticity. Calcium influx through N-methyl-D-aspartate receptors (NMDARs) and Ca<sup>2+</sup>-permeable  $\alpha$ -Amino-3-hydroxy-5-methyl-4-isoxazolepropionic acid receptor (AMPA) drives rapid changes in synaptic efficacy (Liu

and Zukin, 2007; Malenka, 2003) and triggers activity-dependent gene transcription and protein synthesis (Chen et al., 2012b; Nedivi, 1999; Sutton and Schuman, 2006; West and Greenberg, 2011). Activity-regulated protein translation by mRNA-binding proteins provides a mechanism to coordinate expression of a cohort of transcripts (Keene and Tenenbaum, 2002). Studies in hippocampal neuron cultures (Atkins et al., 2004; Wu et al., 1998) and mammalian visual cortex (Wells et al., 2001) suggest that a cascade of NMDAR activation, calcium influx, and  $\alpha$ CaMKII activation result in cytoplasmic polyadenylation element-binding protein (CPEB) phosphorylation and relief of translational inhibition. Although CPEB has been shown to play a role in synaptic plasticity across phyla (Berger-Sweeney et al., 2006; Bestman and Cline, 2008; Dziembowska et al., 2012; Keleman et al., 2007; Oruganty-Das et al., 2012; Richter, 2010; Si et al., 2003; Wells et al., 2001), evidence that it is required for behavioral plasticity in vertebrates is limited (Berger-Sweeney et al., 2006). In the *Xenopus* visual system, NMDAR, CaMKII, and CPEB regulate synaptic strength, experience-dependent structural plasticity, and tectal cell visual responses (Bestman and Cline, 2008; Rajan et al., 1999; Sin et al., 2002; Wu et al., 1996; Wu and Cline, 1998). Recent work has shown that tadpoles exhibit an innate visual avoidance behavior, in which animals avoid an approaching visual stimulus (Dong et al., 2009; Shen et al., 2011); however it is unclear whether the visual avoidance behavior shows experience-dependent plasticity or what cellular mechanisms govern the behavioral plasticity.

Bio-orthogonal metabolic labeling and click chemistry have advanced the study of proteins (Best, 2009; Ngo and Tirrell, 2011; Speers and Cravatt, 2004). Azidohomoalanine (AHA) is a noncanonical amino acid (ncAA) methionine analog that is incorporated into newly synthesized proteins in place of methionine. AHA's highly reactive azide group does not react with functional groups in cells but efficiently reacts with biotin alkyne using copper-catalyzed azide-alkyne cycloaddition (CuAAC) in a click chemistry reaction. Furthermore, the small size of the reactive group does not interfere with protein function and is not toxic to cells or animals (Beatty and Tirrell, 2008; Best, 2009; Dieterich

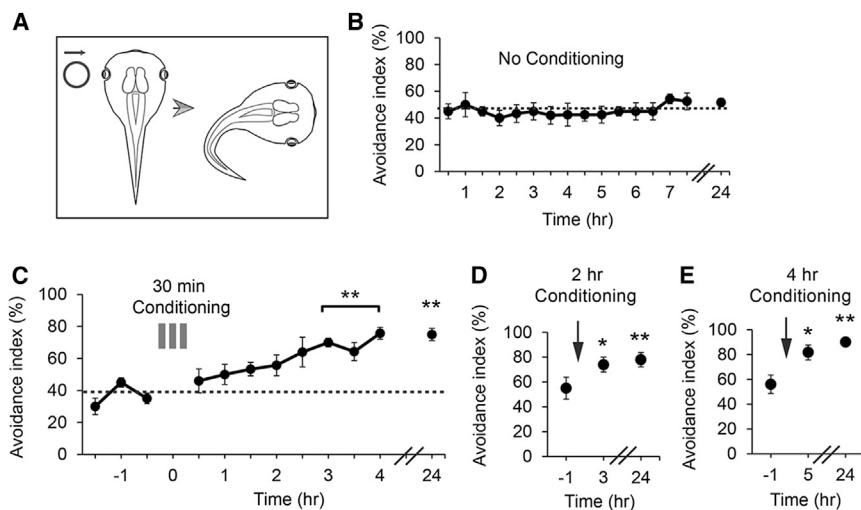


**Figure 1. Conditioning-Dependent Plasticity of Visual Avoidance Behavior**

(A) Diagram of visual avoidance behavior. When a stimulus approaches a freely swimming tadpole, the animal rapidly changes its swim trajectory.

(B) AI remains constant over 7 hr and is unchanged after 24 hr. Dotted line is the average AI over the first three tests.

(C) VC for 30 min during the period marked with the gray bars significantly enhanced AI for at least 24 hr.

(D and E) AI significantly increased compared to baseline when tested up to 24 hr after 2 or 4 hr of VC. Data are presented as mean  $\pm$  SEM. \*\* $p < 0.01$ ; \* $p < 0.05$ .  $n = 6$ –12 animals per group. See also Figure S1.

et al., 2006, 2010; Hinz et al., 2012; Melemedjian et al., 2010; Ngo and Tirrell, 2011; Yang et al., 2010). Because almost all proteins have at least one methionine (97.9% of *Xenopus* transcripts in RefSeq begin with methionine), this method can provide an accurate report of newly synthesized proteins. AHA-biotin-labeled proteins have been detected after AHA exposure in cultured neurons and nonneuronal cells (Beatty and Tirrell, 2008; Choi et al., 2012; Dieterich et al., 2006, 2010; Dziembowska et al., 2012; Melemedjian et al., 2010), and in zebrafish larvae (Hinz et al., 2012, 2013) using western blots or fluorescent noncanonical amino acid tagging (FUNCAT) to detect AHA-labeled proteins; however, direct detection of AHA-biotin-modified peptides by the multidimensional protein identification technique (MudPIT) has been challenging.

Here, we demonstrate that visual conditioning (VC) induces protein synthesis-dependent plasticity of visual avoidance behavior. Using bio-orthogonal nCAA tagging (BONCAT) and MudPIT, we identify  $\sim 1,000$  proteins in the tadpole brain that are synthesized over 24 hr. We also use BONCAT with western blots to identify proteins that are induced in response to VC, including CPEB. Finally, we demonstrate that acute synthesis of CPEB during VC is required for behavioral plasticity and the underlying synaptic and structural plasticity in the tectum. In contrast to the prevailing model that protein synthesis is required for late maintenance phases of plasticity, our data suggest that protein synthesis is required earlier, during induction of plasticity, and identify key players in early protein synthesis-dependent plasticity.

## RESULTS

### Experience-Dependent Plasticity of Visual Avoidance Behavior

Tadpoles escape from an approaching object by changing their swim trajectory when an object approaches the animal at approximately right angles to the eye (Figure 1A). We determined the avoidance index (AI; percentage (%) of avoidance responses per ten trials) in response to 0.4 cm stimuli (Dong et al., 2009; Shen et al., 2011) over 4–24 hr by measuring the AI during

1 min test periods with half an hour intervals between tests. We did not observe any habituation of AI when animals were tested over 7 hr (Figure 1B), indicating that our method is suitable for studies of behavioral plasticity over this time frame. Because tadpoles are not prescreened for high performance of avoidance behavior (Shen et al., 2011), the average AI for control animals is  $\sim 40\%$ , providing the opportunity to detect changes in AI.

We tested whether VC affects visual avoidance behavior by exposing freely swimming animals to a stimulus composed of bars moving at 0.3 Hz in four directions in pseudorandom order and testing visual avoidance. AI was measured three times at 30 min intervals to establish a baseline before tadpoles were exposed to VC. Exposure to 30 min of conditioning consisting of three 5 min episodes of moving bars with 5 min intervals between episodes significantly increased the AI for 24 hr (Figure 1C). Exposure to 2 or 4 hr of continuous VC significantly improved AI when tested 30 min or 1 day after conditioning (Figures 1D and 1E). VC did not significantly affect responses to other stimuli (Figure S1). We used the 30 min VC protocol in the following experiments to investigate mechanisms underlying rapid induction of visual avoidance plasticity.

### NMDAR, $Ca^{2+}$ -Permeable AMPAR, and CaMKII Are Required for Plasticity of Visual Avoidance Behavior

Exposing animals to ( $\pm$ )-3-(2-carboxypiperazin-4-yl)-propyl-1-phosphonic acid (CPP; 25  $\mu$ M), a potent and selective NMDAR antagonist, during but not after VC blocked plasticity of avoidance behavior (Figures 2A and 2B). Exposing tadpoles to Joro Spider Toxin (JST; 500 nM), a specific  $Ca^{2+}$ -permeable GluAR blocker, during or just after VC blocked behavioral plasticity (Figure 2C). Exposure to JST without VC does not affect the AI (Figure S2). Exposing tadpoles to the CaMKII inhibitor KN93 (5  $\mu$ M) during VC blocked behavioral plasticity (Figure 2E), whereas the inactive analog KN92 (5  $\mu$ M) did not (Figure 2F).

### Visual Avoidance Plasticity Requires Protein Synthesis during Conditioning

Protein synthesis is thought to be necessary for late stages of learning and memory (Agranoff and Klinger, 1964; Chen et al.,

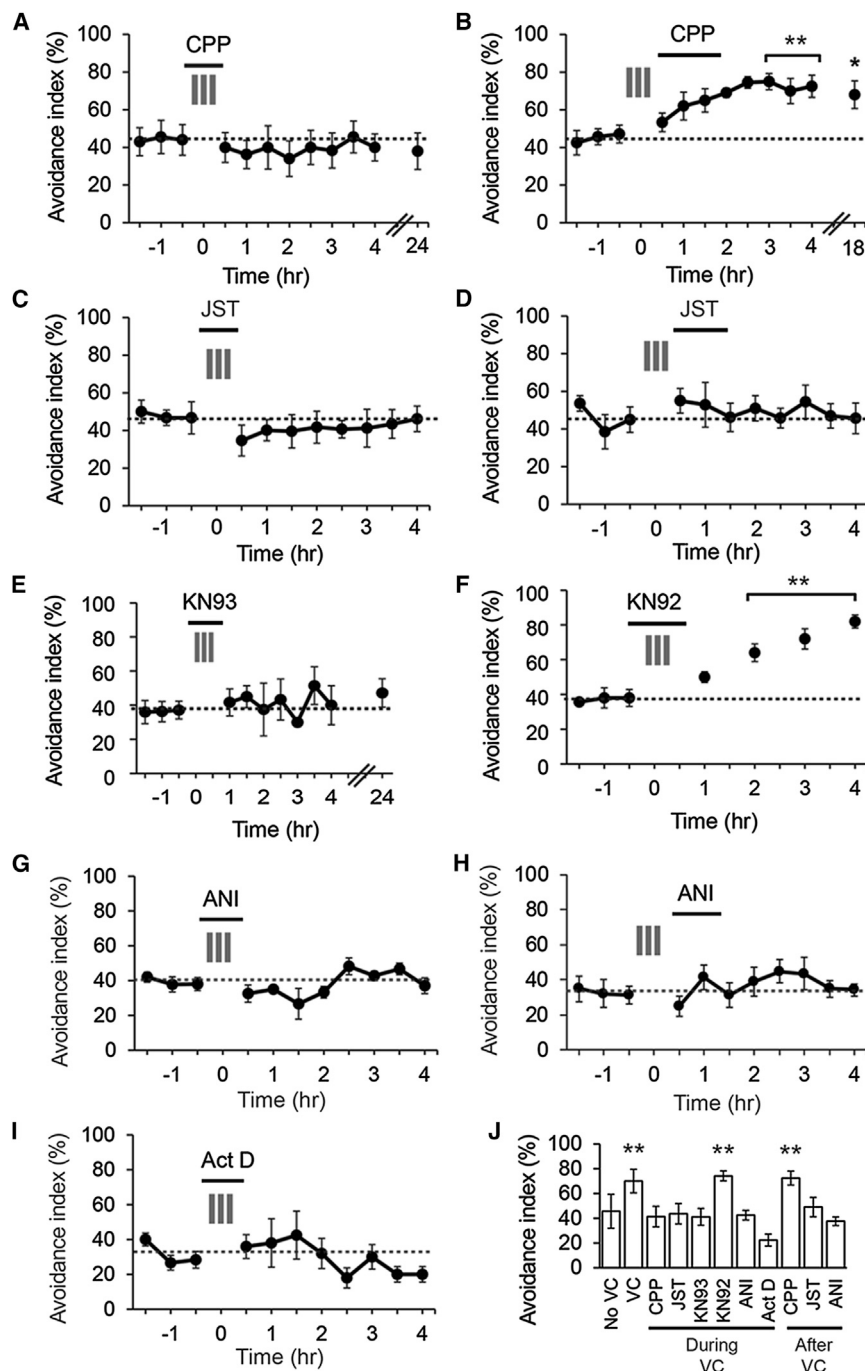


**Figure 2. Behavioral Plasticity Requires Calcium-Dependent Signaling, Gene Transcription, and Protein Synthesis**

(A and B) CPP (25  $\mu$ M) during but not after VC blocked visual avoidance plasticity. (C and D) JST (500 nM) during or after VC blocks behavioral plasticity. (E and F) KN93 (5  $\mu$ M) but not KN92 (5  $\mu$ M) blocks behavioral plasticity. (G and H) ANI (25  $\mu$ M) during or after VC blocks plasticity. (I) Act D (25  $\mu$ M) during VC blocks behavioral plasticity. (J) AI (mean  $\pm$  SEM) from 3 to 4 hr after VC. n = 8–16 animals per group. All data are presented as mean  $\pm$  SEM. \*\*p < 0.01; \*p < 0.05. See also Figure S2.

health or sensorimotor responses. Summary plots of AI measured 3–4 hr after VC show that behavioral plasticity depends on NMDAR, Ca<sup>2+</sup>-permeable AMPAR, and CaMKII, as well as gene transcription and protein translation (Figure 2J).

**Acute Labeling of Newly Synthesized Proteins In Vivo**

We used BONCAT with AHA incorporation to label newly synthesized CNS proteins in intact tadpoles (Figure 3A). Tecta harvested 2 hr after ventricular AHA injection show extensive labeling of biotinylated proteins over a wide range of molecular weights (Figure 3B). Newly synthesized proteins labeled by BONCAT can be detected within 30 min of AHA injection and increase over 3.5 hr (Figure 3C).

To test whether AHA incorporation can be used to detect changes in protein synthesis in vivo, we exposed tadpoles to ANI and to the GABA receptor antagonist, pentylenetetrazol (PTZ). PTZ induces seizure (Hewapathirane et al., 2008), which increases gene expression and protein synthesis (Hinz et al., 2012; Worley et al., 1990). ANI significantly decreased AHA incorporation, and PTZ

significantly increased AHA labeling compared to untreated tadpoles (Figure 3D).

2012b; Flexner et al., 1963; Sutton and Schuman, 2006). Exposing animals to anisomycin (ANI; 25  $\mu$ M), a protein synthesis inhibitor, during or immediately after VC blocked behavioral plasticity (Figures 2G and 2H). Furthermore, exposing animals to actinomycin D (Act D; 25  $\mu$ M), a transcriptional inhibitor, during VC also blocked behavioral plasticity (Figure 2I). Exposing tadpoles to ANI or Act D for 8 hr does not affect the baseline AI (Figure S2), indicating that the short-term drug exposures used here do not alter the animal's

significantly increased AHA labeling compared to untreated tadpoles (Figure 3D).

**MudPIT Analysis of AHA-Biotin-Labeled Newly Synthesized Proteins**

We used MudPIT to analyze newly synthesized proteins in tadpole brains. Stage 47/48 tadpoles received two ventricular AHA injections over 24 hr, and brains were dissected 1–2 hr after the second injection. We optimized the CuAAC click

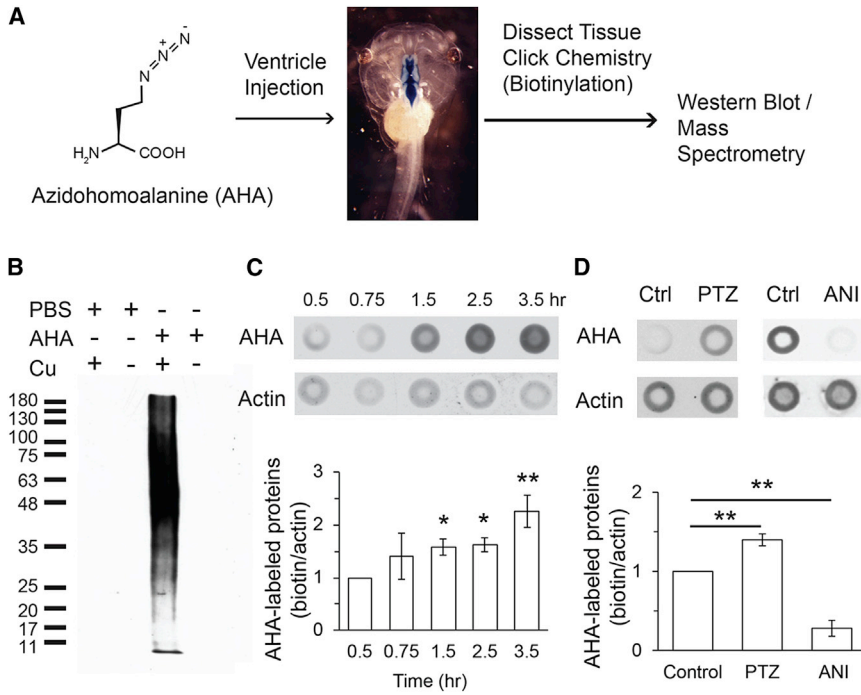


**Figure 3. Rapid Labeling of Newly Synthesized Proteins In Vivo**

(A) Diagram of AHA labeling of newly synthesized proteins and detection by western blot or MudPIT. (B) Newly synthesized proteins detected 2 hr after ventricular AHA injection. PBS injection or click chemistry without copper (Cu) produces minimal labeling.

(C and D) Quantification of AHA labeling. Top panels show dot blots of AHA-biotin label and C4-actin, for normalization. Bottom panels show relative changes in AHA labeling. Whole brains were dissected 3 hr after AHA injection. AHA labeling increases over 3.5 hr after ventricular AHA injection (C). ANI (25  $\mu$ M in rearing solution) significantly decreases AHA labeling, and PTZ (15 mM in rearing solution) significantly increases AHA labeling compared to controls (D; Ctrl). Relative intensity of biotin labeling is  $1.40 \pm 0.07$  for PTZ and  $0.28 \pm 0.10$  for ANI ( $n = 3-5$ ). Data in (C) and (D) are presented as mean  $\pm$  SEM. \*\* $p < 0.01$ ; \* $p < 0.05$ . Ventricular injection of ANI or cycloheximide also decreased AHA labeling compared to PBS-injected controls (Figure S3).

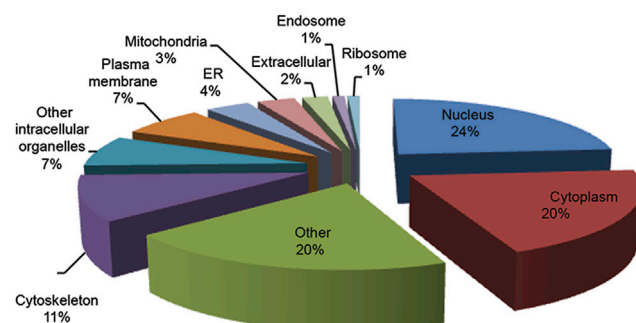
chemistry reaction and established methods to enrich mass spectrometry samples for peptides containing biotinylated AHA. We identified proteins based on direct detection of peptides containing biotinylated AHA by measuring the molecular mass shifts of biotin-modified peptides compared to unmodified peptides to eliminate false-positive calls. From the brains of 1,200–1,500 AHA-injected tadpoles, we detected 992 newly synthesized proteins from 1,617 AHA-biotin-modified peptides. AHA-biotin-labeled proteins were categorized according to the protein's annotated cellular localization using STRAP (Software Tool for Researching Annotations of Proteins) (Bhattia et al., 2009) (Figure 4A; Table S1). The newly synthesized proteins were annotated to a wide variety of cellular compartments, including the nucleus, cytoplasm, and cytoskeleton. We searched our data set for proteins that are functionally related to neural circuit development and plasticity, and present them according to functional categories including translation regulation, protein kinases and phosphatases, receptors, channels, membrane trafficking, and cell adhesion (Figure 4B; Table S2). Key players in synaptic plasticity were AHA labeled, including protein phosphatases and protein kinases, such as CaMKII, MAPK, PI3K, and PKA, synaptic proteins including SNAREs, Homer, oligophrenin, AMPARs and NMDARs, and translational regulators, such as translation initiation and elongation factors, the mRNA-binding proteins, CPEB, staufer, and pumilio, and growth factors including brain-derived neurotrophic factor (BDNF). These data indicate that in vivo BONCAT can be used to identify newly synthesized proteins based on direct detection of AHA-biotin-modified peptides by MudPIT. The data demonstrate the breadth and diversity of the newly synthesized proteome generated over 24 hr in the intact brain.

### Identification of Newly Synthesized Proteins Induced by VC

We exposed AHA-injected animals to VC for 30 min and dissected optic tecta after 2 hr in ambient light. Ventricular injection of 500 mM AHA does not affect visual avoidance behavior or behavioral plasticity (Figure S4), confirming studies in zebrafish (Hinz et al., 2012), indicating that AHA can be used to assess protein synthesis in vivo without interfering with neural circuit function or behavior. Proteins for which antibodies are available were analyzed as shown in Figure 5A. First, we estimated protein levels in an aliquot of the tectal homogenate by measuring  $\beta$ -tubulin by western blot. The remainder of the sample was processed for click chemistry and used to assess newly synthesized AHA-biotin-tagged  $\beta$ -tubulin. The same blots from the click chemistry samples were stripped and labeled with  $\beta$ -tubulin antibody in order to reveal the newly synthesized AHA-biotin-labeled  $\beta$ -tubulin (Figure 5A). Comparable amounts of  $\beta$ -tubulin were detected in samples from control and VC tadpoles (Figure 5A, left), but more newly synthesized AHA-biotin-labeled  $\beta$ -tubulin was detected after VC (Figure 5A, middle and right). These data indicate that BONCAT can dramatically increase the sensitivity to detect changes in protein synthesis.

Analysis of AHA-biotin labeling in candidate proteins showed that VC rapidly increased the synthesis of some proteins, including the protein kinases MEK1 and CaMKII, the histone deacetylase HDAC3, the translational regulator CPEB1, and the GABA synthetic protein GAD65. AHA labeling in other proteins was not changed by VC, including synaptic proteins, syntaxin 1A (STX1A) and SNAP25, the transcription factor CREB, and the cell adhesion molecule cadherin. Finally, AHA incorporation was not detected in several candidates we tested: NF-M, PSD95, and  $\gamma$ 2 subunit of GABA<sub>A</sub> receptors (Figures 5B–5D).

## A Subcellular Localization



## B Biological Processes

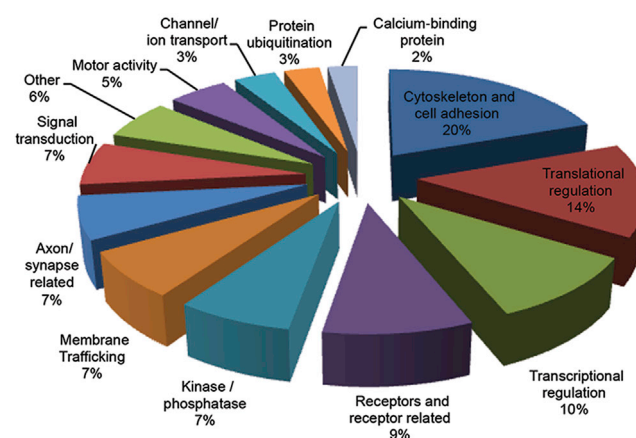


**Figure 4. Mass Spectrometric Analysis of AHA Incorporation In Vivo Identifies Newly Synthesized CNS Proteins**

(A) Annotation of AHA-biotin-labeled proteins according to subcellular compartments and organelles using STRAP. Proteins in each compartment are listed in Table S1.

(B) Annotation of AHA-biotin-labeled proteins according to function in neurons. Proteins are listed in Table S2.

## Visual Avoidance Behavior Is Regulated by CPEB Signaling

We electroporated tadpoles with translation-blocking morpholinos against CPEB (CPEB-MO), which knock down CPEB and decrease CPEB function (Bestman and Cline, 2008), and subjected them to VC 2 days later. Electroporation distributes morpholinos throughout the tectum (Bestman and Cline, 2013). CPEB-MO or control morpholino (Ctrl-MO) did not affect the baseline AI, but CPEB-MO specifically blocked VC-induced visual avoidance plasticity (Figures 6A, 6D, and 6E). Coelectroporating CPEB-MO and morpholino-insensitive *Xenopus* CPEB-CFP increased the baseline AI, which was not affected by CPEB-MO (Figures 6B, 6D, and 6E), suggesting that overexpression of CPEB occluded the effect of VC on behavior. By contrast, coelectroporating mutant CPEB, which lacks the phosphorylation sites required to activate CPEB (Wu et al., 1998), does not affect the baseline AI and blocks the VC-induced

behavioral plasticity (Figures 6C–6E). Data presented in Figure 5 indicate that VC acutely increases CPEB synthesis. Electroporating CPEB-MO immediately before VC blocked behavioral plasticity (Figure 6F), suggesting that newly synthesized CPEB induced during VC is required for plasticity of visuomotor behavior. Consistent with this, CPEB-MO blocks VC-induced CaMKII phosphorylation and decreases VC-induced AHA-CaMKII labeling (Figure S5).

## VC-Dependent Retinotectal Circuit Plasticity Is Blocked by Acute CPEB Knockdown

We recorded visually evoked excitatory compound synaptic currents (CSCs) from tectal neurons in animals with or without VC. Visually evoked retinotectal responses and recurrent tectal circuit activity are significantly greater when recorded 1–3 hr after VC (Figures 7A and 7B). We electroporated tadpoles with CPEB-MO 2 hr before VC and recorded visually evoked responses within 3 hr afterward. Acute CPEB-MO blocked VC-induced potentiation of visually evoked responses (Figures 7A and 7B).

In vivo time-lapse imaging of optic tectal neuronal dendrites shows VC-induced increase in dendritic arbor elaboration (Figure 7C), as previously described by Sin et al. (2002). Electroporating CPEB-MO 2 hr before time-lapse imaging specifically blocked the VC-induced structural plasticity of tectal cell dendrites (Figures 7C and 7D). Together, these data suggest that acutely decreasing CPEB synthesis simultaneously blocks VC-induced tectal cell structural plasticity, synaptic plasticity in retinotectal circuit, and behavioral plasticity.

## DISCUSSION

This study demonstrates that visual avoidance behavior in *Xenopus* is plastic and increases after VC. We demonstrate that a signaling pathway including NMDAR, GluAR, CaMKII, and CPEB is required for VC-induced plasticity of visual avoidance behavior. Furthermore, the behavioral plasticity requires proteins whose synthesis is induced by VC. By combining AHA incorporation, BONCAT, and MudPIT, we identified the newly synthesized brain proteome labeled over 24 hr in the developing brain in vivo. We show that CPEB, CaMKII, MEK1, HDAC3, and GAD65 are among the AHA-labeled proteins whose de novo synthesis is increased in response to VC. Finally, we show that delivery of translation-blocking morpholinos for CPEB immediately prior to conditioning blocks behavioral, synaptic, and structural plasticity in the tectal circuit. We expect that improved strategies we present here to label and identify newly synthesized proteins from the intact brain of behaving animals by MudPIT and western blot will be broadly applicable to a variety of experimental systems and conditions.

## In Vivo Labeling and Screening of Newly Synthesized Proteins

Since the original observations that protein synthesis inhibitors block learning in goldfish and mice (Agranoff and Klinger, 1964; Flexner et al., 1963), considerable effort has been devoted to identify proteins synthesized during plasticity, starting with labeling newly synthesized proteins with radioactive amino acids

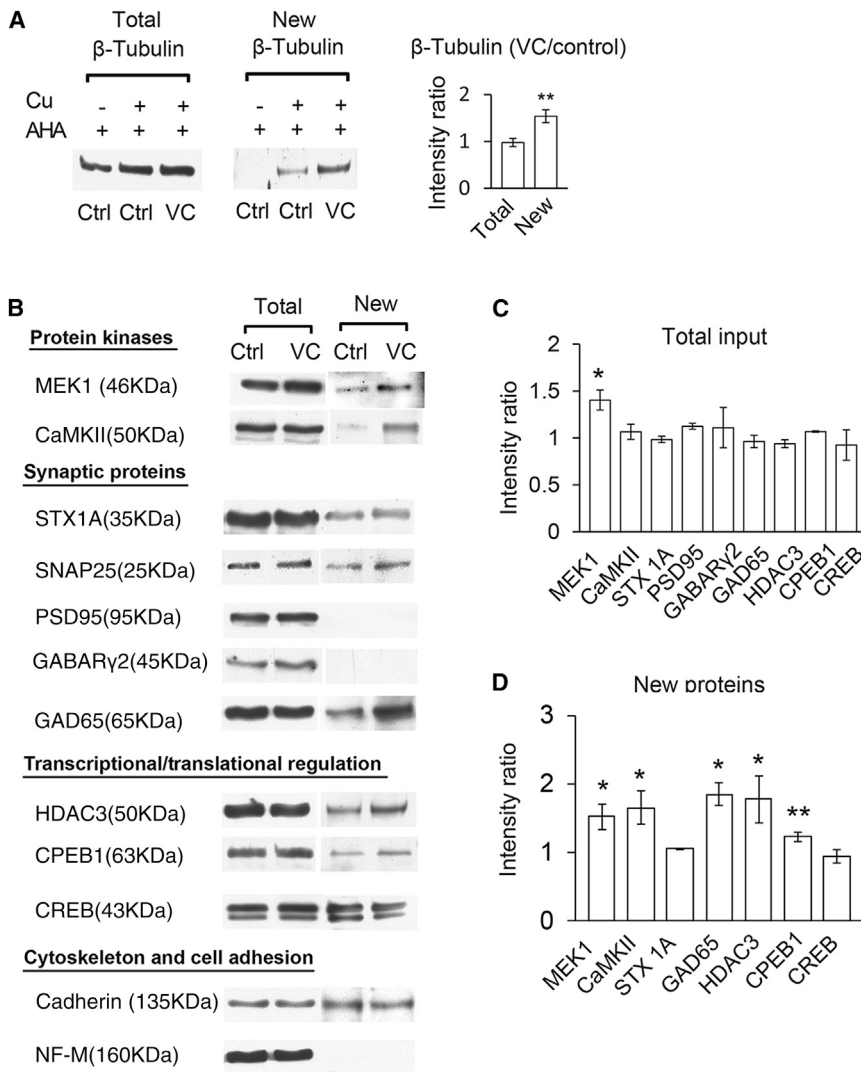


**Figure 5. Identification of Proteins Synthesized in Response to VC**

(A) Analysis of AHA-labeled  $\beta$ -tubulin relative to total  $\beta$ -tubulin in tecta from control and VC tadpoles. Left panel shows that total  $\beta$ -tubulin in control and VC samples is comparable (VC/control,  $0.98 \pm 0.09$ ). Middle and right panels show that VC increases AHA-biotin-labeled  $\beta$ -tubulin (VC/control,  $1.5 \pm 0.2$ ;  $n = 3$ ). AHA-biotin-labeled  $\beta$ -tubulin is not detected when copper is omitted from the reaction.

(B) VC increases protein synthesis. Protein candidates were measured in the total input and as biotinylated proteins from control and VC animals. (C and D) Quantification of data in (B). Relative labeling intensities (VC/control) of total input (C) or AHA-biotin (D) are shown ( $n = 3$  independent experiments for each candidate).

All data are presented as mean  $\pm$  SEM. \* $p < 0.05$ ; \*\* $p < 0.01$ .

of AHA is sufficient to label proteins in vivo within 1–2 hr after injection. The increased temporal resolution of AHA labeling was key to our ability to identify proteins whose synthesis is rapidly regulated by VC.

AHA biotinylation by click chemistry permits enrichment of newly synthesized proteins for subsequent analysis by mass spectrometry (Choi et al., 2012; Hodas et al., 2012). In previous studies, biotinylated proteins were enriched by incubating complex protein mixtures with NeutrAvidin resin. The bound proteins, including biotinylated proteins and proteins that are nonspecifically or indirectly retained on the resin, were digested with protease, and resultant peptides were

(Duffy et al., 1981; Shashoua, 1977a, 1977b). More recent work has used stable isotope labeling with amino acids in cell culture (SILAC) combined with mass spectrometry to identify and quantify differences in brain protein expression (Konzer et al., 2013; Liao et al., 2008); however, isotope labeling for global proteomic analysis does not distinguish newly synthesized proteins from preexisting proteins because they are chemically identical. BONCAT labeling in neurons followed by detection of biotinylated proteins by western blot has permitted gross quantification of global changes in levels of protein synthesis and identification of specific candidate proteins (Dziembowska et al., 2012; Hinz et al., 2012; Hodas et al., 2012).

A previous study in which zebrafish embryos were exposed to 4 mM AHA in embryo medium demonstrated a gradual accumulation of AHA-biotin-labeled proteins over 72 hr (Hinz et al., 2012). To increase the temporal resolution of the AHA labeling and to compete with endogenous methionine, which interferes with AHA incorporation into nascent proteins, we injected 150–500 mM AHA into the brain ventricle. A single ventricular injection

identified by MudPIT. This protocol makes it difficult to identify peptides that are directly modified by the incorporation of the AHA because they are a minority of peptides in the complex mixture applied to tandem mass spectrometry (MS/MS). To address this problem of signal to noise, we performed the biotinylation click reaction with biotin alkyne, which cannot be cleaved by proteases, and digested the protein mixture with trypsin prior to incubation with NeutrAvidin resin. This optimized the enrichment of AHA-biotinylated peptides from the total lysate, resulting in samples in which the majority of peptides identified by MS/MS were directly modified by AHA-biotin. Consequently, our improved sample preparation, together with search algorithms targeted for the mass shift conferred by the AHA-biotin tag, increased our confidence in the identification of newly synthesized proteins by enriching the sample in peptides that included AHA-biotin, by directly identifying the modified peptides, and by excluding false positives from the candidate list that arise by calling proteins based on unmodified peptides.

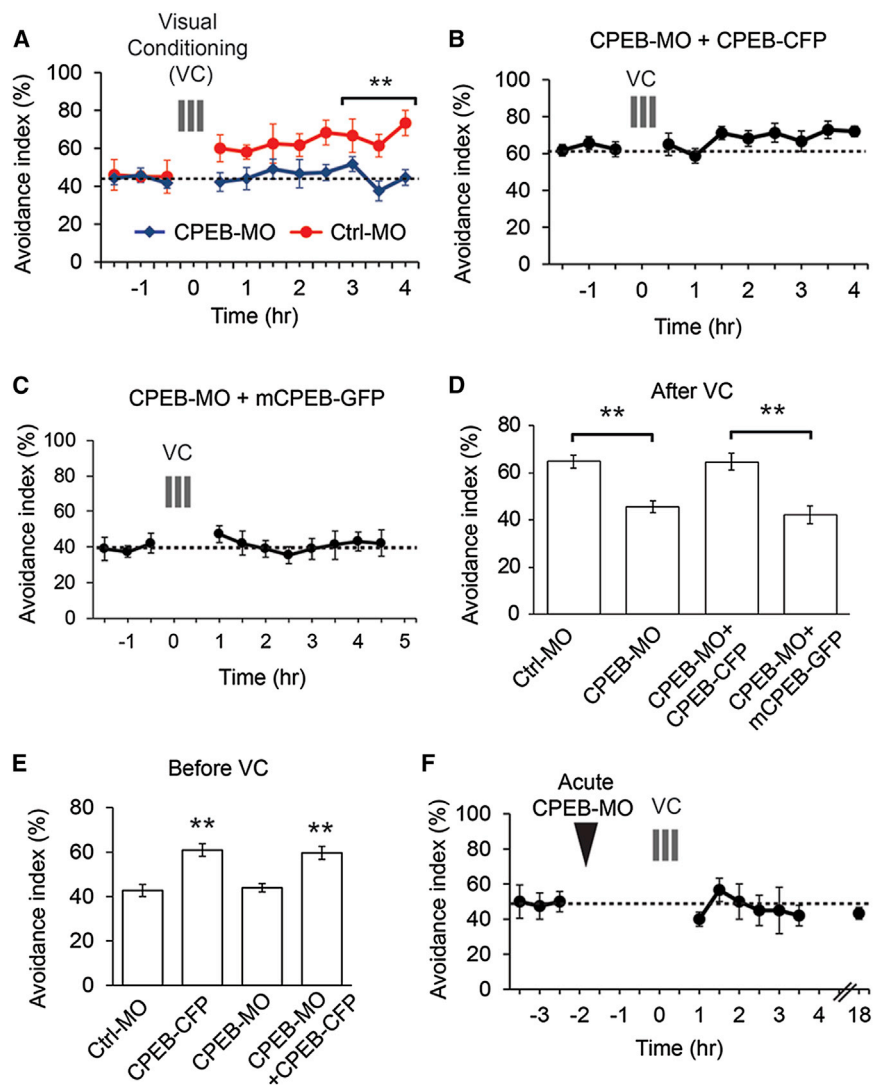


**Figure 6. CPEB Is Required for Plasticity of Avoidance Behavior**

(A) CPEB-MO (blue) blocks VC-induced visual avoidance behavior seen with Ctrl-MO (red). Morpholinos were electroporated 2 days before VC and behavioral testing. (B) Coelectroporation of CPEB-MO and full-length *Xenopus* CPEB-CFP increases the baseline AI and occludes VC-induced plasticity. (C) Coelectroporation of CPEB-MO with mutant *Xenopus* CPEB-GFP, lacking CaMKII phosphorylation sites, fails to rescue the decrease in VC-induced plasticity seen with CPEB-MO alone. (D) The AI 3–4 hr after VC. (E) The baseline AI before VC. (F) CPEB-MO electroporated 2 hr before VC blocks behavioral plasticity for at least 18 hr. n = 8–16 animals per group. Data are presented as mean ± SEM. \*\*p < 0.01. See also Figure S5.

with a predominance of these circuit-assembly events in tadpole brain. These data indicate that even within a relatively short period of 24 hr, cells in the developing CNS support considerable turnover of structural proteins and proteins related to membrane structural dynamics, as well as proteins specifically required for neuronal development and building neural circuits. Of particular interest for this study, we note that synaptic proteins, including neurotransmitter receptors, calcium channels, vesicular transport proteins, and vesicular proteins, such as SNAP25, are AHA labeled, suggesting active assembly and plasticity of synaptic components. Another functional category of AHA-labeled proteins

We identified over 990 proteins labeled by AHA incorporation in the brain. We note that proteins concerned with protein synthesis and degradation are represented in the AHA-labeled protein population, including translational machinery, elongation factors, mRNA-binding proteins, ribosomal proteins, proteasomal proteins, and ubiquitin ligases. This indicates that protein homeostasis itself is under dynamic control by factors controlling protein synthesis and degradation. Many AHA-labeled proteins synthesized within the 24 hr window are cytoskeletal proteins, which are known to play an active role in cell proliferation, the development of neuronal structures, and in structural modifications pertaining to synaptogenesis and synaptic plasticity. Similarly, proteins that regulate membrane dynamics, such as GTPases, were also highly represented in the AHA-labeled sample, consistent with the major structural modifications of neurons, glia, and neural progenitor cells during neuronal development and circuit assembly in the tadpole stages used in this study. Proteins related to axon outgrowth, cell adhesion, and axon guidance are AHA labeled, consistent

relevant to the current study is signaling proteins, including protein kinases, CaMKII, MAP kinases, and protein phosphatases. These data demonstrate that identification of AHA-biotin-labeled proteins provides an overview of cellular processes subject to control by protein homeostasis and also allow targeted evaluation of the role of protein synthesis in specific events such as behavioral plasticity.

### Experience-Dependent Synaptic and Behavioral Plasticity

Here, we show that a tectally mediated behavior, the visual avoidance response, is plastic for at least 24 hr after VC. The 30 min VC protocol is sufficient to induce plasticity and reveals the gradual time course of expression of plasticity. Brief VC also resulted in delayed expression of BDNF-dependent changes in synaptic plasticity and a behavioral readout of increased visual acuity (Schwartz et al., 2011), consistent with the gradual or delayed expression of plasticity that we observe. VC appears to induce plasticity through several activity-regulated transcriptional

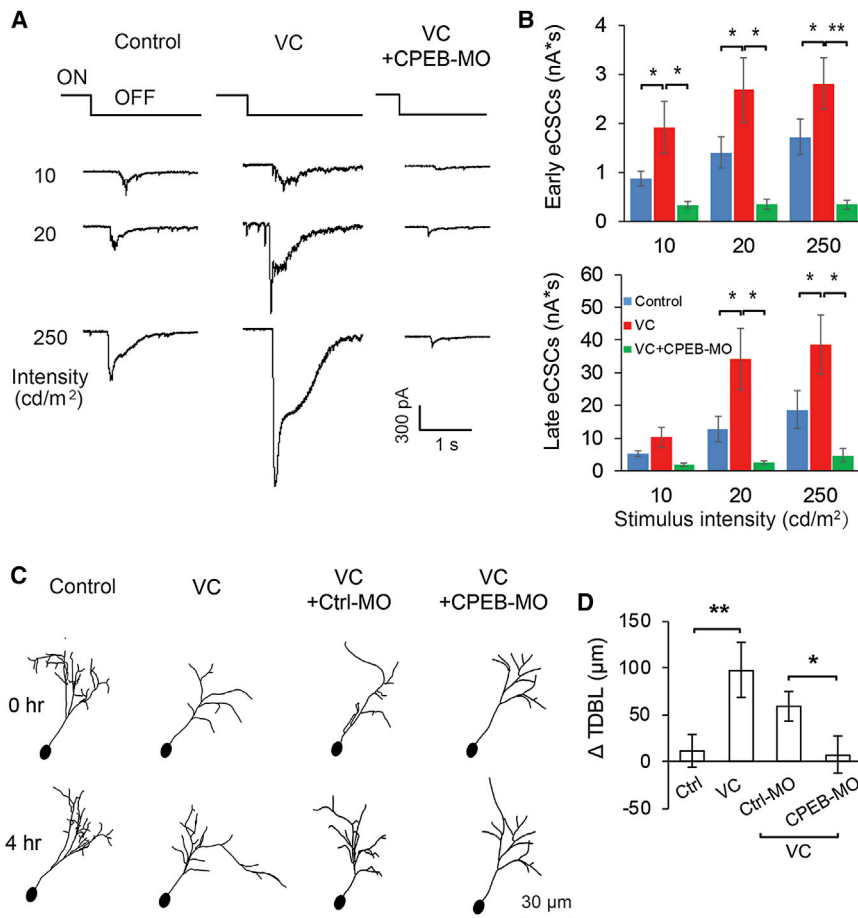


**Figure 7. Conditioning-Dependent Synaptic and Structural Plasticity Requires Acute CPEB Synthesis**

(A) VC-induced excitatory compound synaptic currents (eCSCs) from control, VC, and VC + CPEB-MO animals at light intensities of 10, 20, and 250 cd/m<sup>2</sup>.

(B) VC-induced increases in early (<100 ms) and late (>100 ms) components of CSCs are significantly inhibited by CPEB-MO. Control and Ctrl-MO data were combined because they are not significantly different. MOs were electroporated 2 hr before recording (n = 7–8 neurons/group).

(C) Drawings of representative neurons imaged in vivo over 4 hr in animals exposed to ambient light, VC, VC+Ctrl-MO, and VC+CPEB-MO. MOs were electroporated 2 hr before imaging.

(D) VC significantly increases total dendritic branch length (TDBL) in control and Ctrl-MO neurons, but not in CPEB-MO neurons.

Data are presented as mean ± SEM. \*p < 0.05; \*\*p < 0.01.

pathways (Chen et al., 2012a; Schwartz et al., 2009) and CPEB-mediated translational regulation reported here and previously (Bestman and Cline, 2008), which may operate in parallel. Maintenance of behavioral plasticity was comparable across the different induction protocols, suggesting that comparable plasticity was induced with different VC protocols. Furthermore, VC increases the strength of retinotectal synaptic transmission and recurrent tectal activity (Figure 7), supporting the idea that potentiation of central synapses that process information prior to output to motor systems is a fundamental mechanism of behavioral plasticity.

Numerous studies support a stepwise model in which synaptic activity-mediated membrane depolarization causes a rise in calcium, which in turn activates divergent calcium-dependent signaling pathways that result in both rapid and local changes in synaptic efficacy (Lisman et al., 2012; Malenka, 2003), as well as changes in gene expression and protein synthesis, which in turn affect neural circuit plasticity (West and Greenberg, 2011). In particular, visual avoidance plasticity is induced by a highly conserved signaling pathway for synaptic and behavioral plasticity (Griffith et al., 1993; Lisman et al., 2002; Liu and Zukin, 2007; Man, 2011). Our data showing that application of NMDAR antagonists only during conditioning blocked behavioral plasticity are consistent with the prevailing model of distinct sequential

mechanisms for induction and expression of plasticity. Interestingly, blockade of Ca<sup>2+</sup>-permeable GluAR with JST during or within the first hour after VC inhibited plasticity, suggesting that induction of visual avoidance plasticity includes a sensitive period for calcium influx through GluAR that extends after VC. Calcium entry through GluNR and GluAR engages different downstream signaling pathways, likely reflecting distinct spatiotemporal features of calcium signaling (Man, 2011). In addition, plasticity of transmission through GluNR and GluAR differs (Liu and Zukin, 2007). For instance, VC regulates transmission through Ca<sup>2+</sup>-permeable GluAR by increasing intracellular polyamines (Aizenman et al., 2002), which effectively enhances responses to convergent coactive synaptic inputs by a postsynaptic mechanism of use-dependent relief of polyamine block of Ca<sup>2+</sup>-permeable AMPARs (Bowie and Mayer, 1995; Rozov et al., 1998). Therefore, exposure to JST after VC may block behavioral plasticity by interfering with the enhanced detection of coactive convergent input and resultant signaling from Ca<sup>2+</sup>-permeable GluAR. VC-induced plasticity is mediated by increased retinotectal synaptic transmission, likely due to increased synaptic GluAR trafficking (Haas et al., 2006). Visual experience can also induce persistent neural circuit refinement in a spike timing-dependent manner (Engert et al., 2002; Mu and Poo, 2006; Pratt et al., 2008). Repeated visual stimuli improve visual acuity by a mechanism depending on BDNF-mediated facilitation of retinotectal synapses (Schwartz et al., 2011), consistent with the demonstrated role of BDNF in retinotectal connectivity (Cohen-Cory et al., 2010) and our mass spectrometry results that BDNF is labeled by AHA incorporation. Together, these studies suggest that induction and expression of synaptic and behavioral plasticity in response to VC may operate through highly overlapping and conserved molecular and cellular mechanisms.



### Rapid CPEB Signaling

Our data indicate that VC increased translation of transcripts, including CaMKII, MEK1, and GAD65. Some of the proteins whose synthesis was increased with VC have CPE sites and are likely CPEB targets. Others are likely effector proteins, such as GAD65, a known activity-regulated protein that increases GABA synthesis. Finally, other proteins whose translation is regulated by VC are kinases such as MAP kinase, which themselves are pleiotropic in their influence of synaptic and behavioral plasticity. Importantly, blocking CPEB translation acutely during VC blocks behavioral plasticity, as well as synaptic and structural plasticity. This suggests that protein translation-dependent regulation of plasticity occurs more rapidly than previously thought. Furthermore, based on the conservation of CPEB signaling, our study suggests that rapid temporal control of CPEB function may regulate plasticity in other experimental systems.

### EXPERIMENTAL PROCEDURES

#### Animals and Transfection

All protocols were approved by the Animal Care and Use Committee at The Scripps Research Institute. *Xenopus laevis* tadpoles were purchased and reared as previously described (Bestman and Cline, 2008). Stage 47/48 animals were anesthetized in 0.02% MS-222 (tricaine methanesulfonate; Sigma-Aldrich), and the tectum was electroporated with plasmids (1–2  $\mu\text{g}/\mu\text{l}$ ) or morpholinos (1  $\mu\text{M}$ ) (Haas et al., 2002).

#### Visual Avoidance Assay and VC

The visual avoidance assay was conducted on individual tadpoles as described (Shen et al., 2011) (Supplemental Experimental Procedures).

#### Electrophysiology

In vivo whole-cell recordings of visually evoked responses were collected and analyzed as described (Shen et al., 2011) (Supplemental Experimental Procedures).

#### Imaging

In vivo time-lapse two-photon imaging and analysis were conducted as described (Bestman and Cline, 2008) (Supplemental Experimental Procedures).

#### Click Chemistry and Analysis of AHA Labeling by Western Blots

AHA (L-azidohomoalanine, 150–500 mM [pH 7.4]; AnaSpec) or PBS was injected into the tectal ventricle of anesthetized stage 47/48 tadpoles. Animals recovered from anesthesia for 30 min before they were used for experiments. For analysis of AHA-biotin-tagged proteins by western blots, tecta were dissected from 60–100 anesthetized animals for each group and processed for click chemistry labeling (Dieterich et al., 2007; Speers and Cravatt, 2009; Weerapana et al., 2007), as described in the Supplemental Experimental Procedures.

#### Click Chemistry and Analysis of AHA Labeling by MS/MS

For MS/MS, AHA injections were done once a day for 2 days, and brains of 1,200–1,500 animals were dissected 1–2 hr after the second injection. Brains were homogenized in PBS containing 0.5% SDS in PBS/protease inhibitor (PI; Roche cOmplete ULTRA Tablets, Mini, EDTA-free PI cocktail tablets) followed by sonication with a probe sonicator. Samples were boiled for 10 min at 96°C–100°C and adjusted to 0.2% Triton X-100 and then chilled. For each 400  $\mu\text{l}$  reaction, 1.5 mg of total protein was used with 1.7 mM Triazole ligand (Invitrogen) in 4:1 tBuOH/DMSO (Sigma-Aldrich), 50 mM CuSO<sub>4</sub> (Sigma-Aldrich), 5 mM Biotin Alkyne (Invitrogen), and 50 mM TCEP (Sigma-Aldrich) added in sequence. The reaction proceeded for 1–2 hr at room temperature. Excess reagents were removed with methanol/chloroform precipitation. Precipitated protein (15 mg) was air-dried and resuspended in 100  $\mu\text{l}$  of 0.2% ProteaseMAX

(Promega) and then 100  $\mu\text{l}$  of 8 M urea was added. The solution was reduced with 5 mM TCEP for 20 min at 37°C and then reduced with 10 mM IAA for 20 min in the dark at room temperature. Next, 150  $\mu\text{l}$  of 50 mM ammonium bicarbonate and 2.5  $\mu\text{l}$  of 1% ProteaseMAX were added prior to the addition of 200  $\mu\text{g}$  trypsin. The sample was digested for 3 hr at 37°C in a shaking incubator. The peptides were desalted as previously described by Villén and Gygi (2008) and dried with a SpeedVac prior to AHA peptide enrichment. The peptides were resuspended in 1 ml PBS and incubated with 200  $\mu\text{l}$  NeutrAvidin beads (Pierce) at room temperature for 2 hr. Beads were washed with PBS, and the peptides were eluted with elution buffer (0.1% TFA/0.1% formic acid/70% acetonitrile in H<sub>2</sub>O) for the MS/MS analysis.

#### MudPIT

The eluted AHA-biotin peptides were pressure loaded onto a 250  $\mu\text{m}$  inner diameter (i.d.) capillary with a kasil frit containing 2 cm of 10  $\mu\text{m}$  Jupiter C18 material (Phenomenex) followed by 2 cm of 5  $\mu\text{m}$  PartiSphere strong cation exchanger (Whatman). This loading column was washed with buffer containing 95% water/5% acetonitrile/0.1% formic acid. After washing, a 100  $\mu\text{m}$  i.d. capillary with a 5  $\mu\text{m}$  pulled tip packed with 15 cm of 4  $\mu\text{m}$  Jupiter C18 material was attached to the loading column with a union, and the entire split column (loading column-union-analytical column) was placed inline with an Agilent 1100 quaternary high-performance liquid chromatography (HPLC) column and analyzed using a modified 12-step separation described previously by Washburn et al. (2001). The buffer solutions used were 5% acetonitrile/0.1% formic acid (buffer A), 80% acetonitrile/0.1% formic acid (buffer B), and 500 mM ammonium acetate/5% acetonitrile/0.1% formic acid (buffer C). Step 1 consisted of a 60 min gradient from 0%–100% buffer B. Steps 2–11 had the following profile: 3 min of 100% buffer A, 5 min of X% buffer C, a 10 min gradient from 0%–10% buffer B, and a 105 min gradient from 15%–100% buffer B. The buffer C percentages (X) were 10%, 15%, 20%, 25%, 30%, 35%, 40%, 45%, 50%, and 60%, respectively, for the 12-step analysis. For the final two steps, the gradient contained 5 min of 100% buffer A, 5 min of 100% buffer C, a 10 min gradient from 0% to 15% buffer B, and a 105 min gradient from 15% to 100% buffer B.

As peptides eluted from the microcapillary column, they were electrosprayed directly into an LTQ-OrbitrapXL hybrid mass spectrometer (ThermoFinnigan) with the application of a distal 2.4 kV spray voltage. A cycle of one full MS scan (300–1,600 m/z) at 60,000 $\times$  resolution followed by ten data-dependent IT MS/MS spectra at a 35% normalized collision energy was repeated continuously throughout each step of the multidimensional separation. Application of mass spectrometer scan functions and HPLC solvent gradients was controlled by the Xcaliber data system (Thermo Scientific).

#### Analysis of Tandem Mass Spectra

MS/MS spectra were analyzed using the following software analysis protocol. MS/MS spectra remaining after filtering were searched with the ProLuCID (Rauniyar et al., 2013) against the UniProt *Xenopus laevis* 01-01-2011 concatenated to a decoy database in which the sequence for each entry in the original database was reversed (Peng et al., 2003). All searches were parallelized and performed on a Beowulf computer cluster consisting of 100 1.2 GHz Athlon CPUs (Sadygov et al., 2002). A static modification of 57.02146 on cysteine and a differential modification of 523.2749 on methionine were searched. ProLuCID results were assembled and filtered using the DTASelect (version 2.0) program (Cociorva et al., 2007; Tabb et al., 2002). DTASelect 2.0 uses a linear-discriminant analysis to dynamically set XCorr and DeltaCN thresholds for the entire data set to achieve a user-specified false discovery rate (FDR). In addition, the modified peptides were required to be fully tryptic, less than 5 ppm deviation from peptide match, and a FDR at the spectra level of 0.01. The FDRs are estimated by the program from the number and quality of spectral matches to the decoy database. For this analysis, the AHA-modified protein and peptide FDRs were 0.81 and 0.49, respectively. Raw data are available at [http://uther.scripps.edu/published/AHA\\_invivo\\_Xenopus/raws/](http://uther.scripps.edu/published/AHA_invivo_Xenopus/raws/) and can be accessed with Xcalibur 1.0 software for use with Thermo Scientific mass spectrometers. Cellular localization as annotated by Gene Ontology was determined by STRAP (Bhatia et al., 2009). Figure 4 represents the percentage of genes with annotated localizations, and some genes were annotated to multiple compartments.

### Statistical Tests

All data are presented as mean  $\pm$  SEM. Data are considered significantly different when *p* values are less than 0.05. Where noted, two-tailed Student's *t* test was used for comparisons of two groups, and ANOVA with Newman-Keuls test was used for comparisons of multiple groups. Experiments and analyses were performed blind to the experimental conditions.

### SUPPLEMENTAL INFORMATION

Supplemental Information includes Supplemental Experimental Procedures, five figures, and two tables and can be found with this article online at <http://dx.doi.org/10.1016/j.celrep.2014.01.024>.

### ACKNOWLEDGMENTS

We thank Dr. Ben Cravatt and Jonathan Hulse for help optimizing the click chemistry. The work was supported by NIH EY011261, MH 91676 and MH099799, Dart Neuroscience, LLC, the Nancy Lurie Marks Family Foundation, an endowment from the Hahn Family Foundation to H.T.C., MH067880 and P41 GM103533 to J.R.Y., and the National Nature Sciences Foundation of China (NSFC 31271176) to W.S.

Received: March 12, 2013

Revised: December 30, 2013

Accepted: January 15, 2014

Published: February 13, 2014

### REFERENCES

- Agranoff, B.W., and Klinger, P.D. (1964). Puromycin effect on memory fixation in the goldfish. *Science* **146**, 952–953.
- Aizenman, C.D., Muñoz-Eliás, G., and Cline, H.T. (2002). Visually driven modulation of glutamatergic synaptic transmission is mediated by the regulation of intracellular polyamines. *Neuron* **34**, 623–634.
- Atkins, C.M., Nozaki, N., Shigeri, Y., and Soderling, T.R. (2004). Cytoplasmic polyadenylation element binding protein-dependent protein synthesis is regulated by calcium/calmodulin-dependent protein kinase II. *J. Neurosci.* **24**, 5193–5201.
- Beatty, K.E., and Tirrell, D.A. (2008). Two-color labeling of temporally defined protein populations in mammalian cells. *Bioorg. Med. Chem. Lett.* **18**, 5995–5999.
- Berger-Sweeney, J., Zearfoss, N.R., and Richter, J.D. (2006). Reduced extinction of hippocampal-dependent memories in CPEB knockout mice. *Learn. Mem.* **13**, 4–7.
- Best, M.D. (2009). Click chemistry and bioorthogonal reactions: unprecedented selectivity in the labeling of biological molecules. *Biochemistry* **48**, 6571–6584.
- Bestman, J.E., and Cline, H.T. (2008). The RNA binding protein CPEB regulates dendrite morphogenesis and neuronal circuit assembly in vivo. *Proc. Natl. Acad. Sci. USA* **105**, 20494–20499.
- Bestman, J.E., and Cline, H.T. (2013). Application of antisense morpholino oligonucleotides to study *Xenopus* brain development and plasticity. In *Brain Development*, S. Schecter, ed. (New York: Springer).
- Bhatia, V.N., Perlman, D.H., Costello, C.E., and McComb, M.E. (2009). Software tool for researching annotations of proteins: open-source protein annotation software with data visualization. *Anal. Chem.* **81**, 9819–9823.
- Bowie, D., and Mayer, M.L. (1995). Inward rectification of both AMPA and kainate subtype glutamate receptors generated by polyamine-mediated ion channel block. *Neuron* **15**, 453–462.
- Chen, S.X., Cherry, A., Tari, P.K., Podgorski, K., Kwong, Y.K., and Haas, K. (2012a). The transcription factor MEF2 directs developmentally driven functional and structural metaplasticity. *Cell* **151**, 41–55.
- Chen, C.C., Wu, J.K., Lin, H.W., Pai, T.P., Fu, T.F., Wu, C.L., Tully, T., and Chiang, A.S. (2012b). Visualizing long-term memory formation in two neurons of the *Drosophila* brain. *Science* **335**, 678–685.
- Choi, K.Y., Lippert, D.N., Ezzatti, P., and Mookherjee, N. (2012). Defining TNF- $\alpha$  and IL-1 $\beta$  induced nascent proteins: combining bio-orthogonal non-canonical amino acid tagging and proteomics. *J. Immunol. Methods* **382**, 189–195.
- Cociorva, D., L Tabb, D., and Yates, J.R. (2007). Validation of tandem mass spectrometry database search results using DTASelect. *Curr. Protoc. Bioinformatics Chapter 13*, Unit 13.4.
- Cohen-Cory, S., Kidane, A.H., Shirkey, N.J., and Marshak, S. (2010). Brain-derived neurotrophic factor and the development of structural neuronal connectivity. *Dev. Neurobiol.* **70**, 271–288.
- Dieterich, D.C., Link, A.J., Graumann, J., Tirrell, D.A., and Schuman, E.M. (2006). Selective identification of newly synthesized proteins in mammalian cells using bioorthogonal noncanonical amino acid tagging (BONCAT). *Proc. Natl. Acad. Sci. USA* **103**, 9482–9487.
- Dieterich, D.C., Lee, J.J., Link, A.J., Graumann, J., Tirrell, D.A., and Schuman, E.M. (2007). Labeling, detection and identification of newly synthesized proteomes with bioorthogonal non-canonical amino-acid tagging. *Nat. Protoc.* **2**, 532–540.
- Dieterich, D.C., Hodas, J.J., Gouzer, G., Shadrin, I.Y., Ngo, J.T., Triller, A., Tirrell, D.A., and Schuman, E.M. (2010). In situ visualization and dynamics of newly synthesized proteins in rat hippocampal neurons. *Nat. Neurosci.* **13**, 897–905.
- Dong, W., Lee, R.H., Xu, H., Yang, S., Pratt, K.G., Cao, V., Song, Y.K., Nurmikko, A., and Aizenman, C.D. (2009). Visual avoidance in *Xenopus* tadpoles is correlated with the maturation of visual responses in the optic tectum. *J. Neurophysiol.* **101**, 803–815.
- Duffy, C., Teyler, T.J., and Shashoua, V.E. (1981). Long-term potentiation in the hippocampal slice: evidence for stimulated secretion of newly synthesized proteins. *Science* **212**, 1148–1151.
- Dziembowska, M., Milek, J., Janusz, A., Rejmak, E., Romanowska, E., Gorkiewicz, T., Tiron, A., Bramham, C.R., and Kaczmarek, L. (2012). Activity-dependent local translation of matrix metalloproteinase-9. *J. Neurosci.* **32**, 14538–14547.
- Engert, F., Tao, H.W., Zhang, L.I., and Poo, M.M. (2002). Moving visual stimuli rapidly induce direction sensitivity of developing tectal neurons. *Nature* **419**, 470–475.
- Flexner, J.B., Flexner, L.B., and Stellar, E. (1963). Memory in mice as affected by intracerebral puromycin. *Science* **141**, 57–59.
- Griffith, L.C., Verselis, L.M., Aitken, K.M., Kyriacou, C.P., Danho, W., and Greenspan, R.J. (1993). Inhibition of calcium/calmodulin-dependent protein kinase in *Drosophila* disrupts behavioral plasticity. *Neuron* **10**, 501–509.
- Haas, K., Jensen, K., Sin, W.C., Foa, L., and Cline, H.T. (2002). Targeted electroporation in *Xenopus* tadpoles in vivo—from single cells to the entire brain. *Differentiation* **70**, 148–154.
- Haas, K., Li, J., and Cline, H.T. (2006). AMPA receptors regulate experience-dependent dendritic arbor growth in vivo. *Proc. Natl. Acad. Sci. USA* **103**, 12127–12131.
- Hewapathirane, D.S., Dunfield, D., Yen, W., Chen, S., and Haas, K. (2008). In vivo imaging of seizure activity in a novel developmental seizure model. *Exp. Neurol.* **211**, 480–488.
- Hinz, F.I., Dieterich, D.C., Tirrell, D.A., and Schuman, E.M. (2012). Non-canonical amino acid labeling in vivo to visualize and affinity purify newly synthesized proteins in larval zebrafish. *ACS Chem Neurosci* **3**, 40–49.
- Hinz, F.I., Aizenberg, M., Tushev, G., and Schuman, E.M. (2013). Protein synthesis-dependent associative long-term memory in larval zebrafish. *J. Neurosci.* **33**, 15382–15387.
- Hodas, J.J., Nehring, A., Höche, N., Sweredoski, M.J., Pielot, R., Hess, S., Tirrell, D.A., Dieterich, D.C., and Schuman, E.M. (2012). Dopaminergic modulation of the hippocampal neuropil proteome identified by bioorthogonal noncanonical amino acid tagging (BONCAT). *Proteomics* **12**, 2464–2476.
- Keene, J.D., and Tenenbaum, S.A. (2002). Eukaryotic mRNPs may represent posttranscriptional operons. *Mol. Cell* **9**, 1161–1167.

- Keleman, K., Krüttner, S., Alenius, M., and Dickson, B.J. (2007). Function of the *Drosophila* CPEB protein Orb2 in long-term courtship memory. *Nat. Neurosci.* *10*, 1587–1593.
- Konzer, A., Ruhs, A., Braun, H., Jungblut, B., Braun, T., and Krüger, M. (2013). Stable isotope labeling in zebrafish allows in vivo monitoring of cardiac morphogenesis. *Mol. Cell. Proteomics* *12*, 1502–1512.
- Liao, L., Park, S.K., Xu, T., Vanderklish, P., and Yates, J.R., 3rd. (2008). Quantitative proteomic analysis of primary neurons reveals diverse changes in synaptic protein content in *fmr1* knockout mice. *Proc. Natl. Acad. Sci. USA* *105*, 15281–15286.
- Lisman, J., Schulman, H., and Cline, H. (2002). The molecular basis of CaMKII function in synaptic and behavioural memory. *Nat. Rev. Neurosci.* *3*, 175–190.
- Lisman, J., Yasuda, R., and Raghavachari, S. (2012). Mechanisms of CaMKII action in long-term potentiation. *Nat. Rev. Neurosci.* *13*, 169–182.
- Liu, S.J., and Zukin, R.S. (2007). Ca<sup>2+</sup>-permeable AMPA receptors in synaptic plasticity and neuronal death. *Trends Neurosci.* *30*, 126–134.
- Malenka, R.C. (2003). Synaptic plasticity and AMPA receptor trafficking. *Ann. N Y Acad. Sci.* *1003*, 1–11.
- Man, H.Y. (2011). GluA2-lacking, calcium-permeable AMPA receptors—inducers of plasticity? *Curr. Opin. Neurobiol.* *21*, 291–298.
- Melemedjian, O.K., Asiedu, M.N., Tillu, D.V., Peebles, K.A., Yan, J., Ertz, N., Dussor, G.O., and Price, T.J. (2010). IL-6- and NGF-induced rapid control of protein synthesis and nociceptive plasticity via convergent signaling to the eIF4F complex. *J. Neurosci.* *30*, 15113–15123.
- Mu, Y., and Poo, M.M. (2006). Spike timing-dependent LTP/LTD mediates visual experience-dependent plasticity in a developing retinotectal system. *Neuron* *50*, 115–125.
- Nedivi, E. (1999). Molecular analysis of developmental plasticity in neocortex. *J. Neurobiol.* *41*, 135–147.
- Ngo, J.T., and Tirrell, D.A. (2011). Noncanonical amino acids in the interrogation of cellular protein synthesis. *Acc. Chem. Res.* *44*, 677–685.
- Oruganty-Das, A., Ng, T., Udagawa, T., Goh, E.L., and Richter, J.D. (2012). Translational control of mitochondrial energy production mediates neuron morphogenesis. *Cell Metab.* *16*, 789–800.
- Peng, J., Elias, J.E., Thoreen, C.C., Licklider, L.J., and Gygi, S.P. (2003). Evaluation of multidimensional chromatography coupled with tandem mass spectrometry (LC/LC-MS/MS) for large-scale protein analysis: the yeast proteome. *J. Proteome Res.* *2*, 43–50.
- Pratt, K.G., Dong, W., and Aizenman, C.D. (2008). Development and spike timing-dependent plasticity of recurrent excitation in the *Xenopus* optic tectum. *Nat. Neurosci.* *11*, 467–475.
- Rajan, I., Witte, S., and Cline, H.T. (1999). NMDA receptor activity stabilizes presynaptic retinotectal axons and postsynaptic optic tectal cell dendrites in vivo. *J. Neurobiol.* *38*, 357–368.
- Rauniyar, N., McClatchy, D.B., and Yates, J.R., 3rd. (2013). Stable isotope labeling of mammals (SILAM) for in vivo quantitative proteomic analysis. *Methods* *61*, 260–268.
- Richter, J.D. (2010). Translational control of synaptic plasticity. *Biochem. Soc. Trans.* *38*, 1527–1530.
- Rozov, A., Zilberter, Y., Wollmuth, L.P., and Burnashev, N. (1998). Facilitation of currents through rat Ca<sup>2+</sup>-permeable AMPA receptor channels by activity-dependent relief from polyamine block. *J. Physiol.* *511*, 361–377.
- Sadygov, R.G., Eng, J., Durr, E., Saraf, A., McDonald, H., MacCoss, M.J., and Yates, J.R., 3rd. (2002). Code developments to improve the efficiency of automated MS/MS spectra interpretation. *J. Proteome Res.* *1*, 211–215.
- Schwartz, N., Schohl, A., and Ruthazer, E.S. (2009). Neural activity regulates synaptic properties and dendritic structure in vivo through calcineurin/NFAT signaling. *Neuron* *62*, 655–669.
- Schwartz, N., Schohl, A., and Ruthazer, E.S. (2011). Activity-dependent transcription of BDNF enhances visual acuity during development. *Neuron* *70*, 455–467.
- Shashoua, V.E. (1977a). Brain protein metabolism and the acquisition of new behaviors. II. Immunological studies of the alpha, beta and gamma proteins of goldfish brain. *Brain Res.* *122*, 113–124.
- Shashoua, V.E. (1977b). Brain protein metabolism and the acquisition of new patterns of behavior. *Proc. Natl. Acad. Sci. USA* *74*, 1743–1747.
- Shen, W., McKeown, C.R., Demas, J.A., and Cline, H.T. (2011). Inhibition to excitation ratio regulates visual system responses and behavior in vivo. *J. Neurophysiol.* *106*, 2285–2302.
- Si, K., Giustetto, M., Etkin, A., Hsu, R., Janisiewicz, A.M., Miniaci, M.C., Kim, J.H., Zhu, H., and Kandel, E.R. (2003). A neuronal isoform of CPEB regulates local protein synthesis and stabilizes synapse-specific long-term facilitation in aplysia. *Cell* *115*, 893–904.
- Sin, W.C., Haas, K., Ruthazer, E.S., and Cline, H.T. (2002). Dendrite growth increased by visual activity requires NMDA receptor and Rho GTPases. *Nature* *419*, 475–480.
- Speers, A.E., and Cravatt, B.F. (2004). Profiling enzyme activities in vivo using click chemistry methods. *Chem. Biol.* *11*, 535–546.
- Speers, A.E., and Cravatt, B.F. (2009). Activity-based protein profiling (ABPP) and click chemistry (CC)-ABPP by MudPIT mass spectrometry. *Curr. Protoc. Chem. Biol.* *1*, 29–41.
- Sutton, M.A., and Schuman, E.M. (2006). Dendritic protein synthesis, synaptic plasticity, and memory. *Cell* *127*, 49–58.
- Tabb, D.L., McDonald, W.H., and Yates, J.R., 3rd. (2002). DTASelect and Contrast: tools for assembling and comparing protein identifications from shotgun proteomics. *J. Proteome Res.* *1*, 21–26.
- Villén, J., and Gygi, S.P. (2008). The SCX/IMAC enrichment approach for global phosphorylation analysis by mass spectrometry. *Nat. Protoc.* *3*, 1630–1638.
- Washburn, M.P., Wolters, D., and Yates, J.R., 3rd. (2001). Large-scale analysis of the yeast proteome by multidimensional protein identification technology. *Nat. Biotechnol.* *19*, 242–247.
- Weerapana, E., Speers, A.E., and Cravatt, B.F. (2007). Tandem orthogonal proteolysis-activity-based protein profiling (TOP-ABPP)—a general method for mapping sites of probe modification in proteomes. *Nat. Protoc.* *2*, 1414–1425.
- Wells, D.G., Dong, X., Quinlan, E.M., Huang, Y.S., Bear, M.F., Richter, J.D., and Fallon, J.R. (2001). A role for the cytoplasmic polyadenylation element in NMDA receptor-regulated mRNA translation in neurons. *J. Neurosci.* *21*, 9541–9548.
- West, A.E., and Greenberg, M.E. (2011). Neuronal activity-regulated gene transcription in synapse development and cognitive function. *Cold Spring Harb. Perspect. Biol.* *3*, a005744.
- Worley, P.F., Cole, A.J., Murphy, T.H., Christy, B.A., Nakabeppu, Y., and Baraban, J.M. (1990). Synaptic regulation of immediate-early genes in brain. *Cold Spring Harb. Symp. Quant. Biol.* *55*, 213–223.
- Wu, G.Y., and Cline, H.T. (1998). Stabilization of dendritic arbor structure in vivo by CaMKII. *Science* *279*, 222–226.
- Wu, G., Malinow, R., and Cline, H.T. (1996). Maturation of a central glutamatergic synapse. *Science* *274*, 972–976.
- Wu, L., Wells, D., Tay, J., Mendis, D., Abbott, M.A., Barnitt, A., Quinlan, E., Heynen, A., Fallon, J.R., and Richter, J.D. (1998). CPEB-mediated cytoplasmic polyadenylation and the regulation of experience-dependent translation of alpha-CaMKII mRNA at synapses. *Neuron* *21*, 1129–1139.
- Yang, Y.Y., Grammel, M., Raghavan, A.S., Charron, G., and Hang, H.C. (2010). Comparative analysis of cleavable azobenzene-based affinity tags for bio-orthogonal chemical proteomics. *Chem. Biol.* *17*, 1212–1222.